Shahrood University of Technology
Iranian Society of Mining Engineering (IRSME)
Journal of Mining and Environment (JME)
journal homepage: www.jme.shahroodut.ac.ir
THOMSON REUTERS
Vol. 11, No. 2, 2020, 629-641.
DOI: 10.22044/jme.2020.9039.1791

3D Characterization of Uniaxial Compressive Strength of Transversely-Isotropic Intact Rocks

V. Maazallahi and A. Majdi*

School of Mining Engineering, College of Engineering, University of Tehran, Tehran, Iran

Received 19 October 2019; received in revised form 30 March 2020; accepted 20 April 2020

Keywords

Intact rock

UCS, Transversely-isotropic

3D characterization

Stereonet

Abstract

The uniaxial compressive strength (UCS) of intact rocks is one of the key parameters in the course of site characterizations. The isotropy/anisotropy condition of the UCS of intact rocks is dependent on the internal structure of the rocks. The rocks with a random grain structure exhibit an isotropic behavior. However, the rocks with a linear/planar grain structure generally behave transversely-isotropic. In the latter case, the UCS of intact rocks must be determined by a set of laboratory tests on the oriented rock samples. There are some empirical relations available to describe the strength of these rocks. Though characterization of transversely-isotropic rocks is practically a 3D problem, but these relations provide only a 2D description. In this paper, a method is proposed to provide a 3D description of UCS of transversely-isotropic rocks. By means of this formulation, one can determine UCS along with any arbitrary spatial direction. Also, a representative illustration of UCS is proposed in the form of contour-plots on a lower hemisphere Stereonet. The method is applied to an actual case study from the Kanigoizhan dam site located in the Kurdistan Province (Iran). Application of the proposed method to the phyllite rocks of this site show that the direction perpendicular to the dam axis exhibits the most anisotropic behavior. Hence, it is essential to take the strength anisotropy into account during the relevant analysis. The results obtained, together with the statistical variation of UCS, provide a practical approach to select the proper values of UCS according to the scope of the analysis.

1. Introduction

Most rocks have some structural defects such as bedding planes, foliations, fracturing, and joints. The presence of these defects leads to a significant change in the strength properties in different directions, known as anisotropy. Anisotropy is observed in different scales, from small intact rock specimens to blocks of jointed rock masses. This phenomenon plays an important role in various earthwork engineering activities such as rock slope stability [1–3] and the stability of underground openings [4, 5]. In such cases, the differences in the mechanical properties of the rock media in different directions can affect the behavior of the aforementioned structures.

Anisotropy may be due to either the intrinsic nature of the rock or the extrinsic factors such as the environmental effects. The primary factors are associated with the origin of the rock; in other words, the weak planes are related to the rock formation processes (e.g. foliation, schistosity, and cleavages). The secondary factors include the existence of fractures and sequences of different rock layers. The anisotropy caused due to the internal structure of intact rocks is termed as intrinsic or inherent anisotropy, which is dealt with in this paper.

Almost all rocks, to some extent, are anisotropic in their mechanical properties [6]; basically, intact rocks with random grain structures (Figure 1a) behave as isotropic, whilst rocks with linear or planar grain structures (Figure 1b) are likely to behave anisotropically in strength and

Corresponding author: amajdi@ut.ac.ir (A. Majdi).

deformability [7]. For example, the rocks such as sandstone and conglomerate that have a random grain structure indicate a low strength anisotropy, while the schistose rocks such as schists and shales that have planar grain structures are generally known as highly anisotropic. The latter case of grain structure commonly leads to a transversely-isotropic behavior. Existence of a set of structural planes that are called 'isotropic planes' is the characteristic of the transversely-isotropic rocks. Parallel to these planes, the strength and deformability are the same and isotropic in all directions. However, they often exhibit a different strength and deformability in directions at different angels relative to the isotropic planes.

Figure 1. Examples of rocks (a) with random grain structures, (b) with planar grain structures. (Pictures of rock cores taken from Kerman water conveyance tunnel, Kerman, Iran.)

The uniaxial compressive strength (UCS) of intact rocks is a key parameter in the course of site characterizations. Many researchers have studied the strength behavior of anisotropic and transversely-isotropic rocks, where the followings are noticeable: Donath [8], Hoek [9], McLamore and Gray [10], Attewell and Sandford [11], and Brown *et al*. [12] on shales and slates, McCabe and Koerner [13], Nasseri *et al*. [14, 15], Singh *et al*. [16], Saroglou and Tsiambaos [17] on gneisses and schists, Ramamurthy *et al*. [18] on phyllites, Al-Harthi [19], Colak and Unlu [20] on sandstones, Ajalloeian and Lashkaripour [21] on mudstone and siltstone. Based on these studies, some fundamental relationships have been proposed to describe the dependency of UCS of intact rocks to the angle of orientation of isotropic planes. Field characterization of UCS of anisotropic rocks requires a 3D development of these relationships. Hence, in this work, a formulation has been developed for calculation of UCS of intact rocks along with any arbitrary direction within the 3D space. This formulation is also capable to yield the all-round spatial distribution of UCS. Subsequently, a representative illustration of UCS has been proposed in the form of its contour-plots on the Stereonet.

2. Strength anisotropy of intact rocks

2.1. Types of inherent anisotropy

The anisotropy of rocks can be categorized based on the shape of the uniaxial compressive strength, $\sigma_{c\beta}$, curve relative to the angle between the weakness planes of the specimen and the maximum applied stress, β. This classification identifies two kinds of anisotropy [22]: a) Cleavage or planar, and b) Bedding plane. This classification is based on three factors: maximum and minimum $\sigma_{c\beta}$ at β = 0ºto 90º, and the shape of the anisotropy curve ($\sigma_{c\beta}$ *vs.* β). The details of this classification are summarized in Table 1. The variations of the uniaxial compressive strength of intact rock versus β for different types of anisotropy are demonstrated in Figure 2.

Table 1. Classification of types of inherent anisotropy (the information extracted from [22, 23]).

Type of anisotropy	Origin	Type of structural defects	Shape and characteristics of anisotropy curve	Example
Bedding plane anisotropy	Sedimentary rocks	Existence of bedding planes	Shoulder type max. $\sigma_{c\beta}$ at β = 0 min. $\sigma_{c\beta}$ at β = 20-40 (see Figure 2-curve I)	Sandstone and shale
Cleavage or planar anisotropy	Metamorphic and chemical rocks whose particles crystallized in specific directions	One set of cleavage	U-shaped $\sigma_{c\beta}$ at β = 90 is greater than β = 0 (see Figure 2-curve II)	Slates
		More than one set of cleavage	Wavy $\sigma_{c\beta}$ at β = 90 is greater than β = 0 (see Figure 2-curve III)	Coal, biochemical diatomite

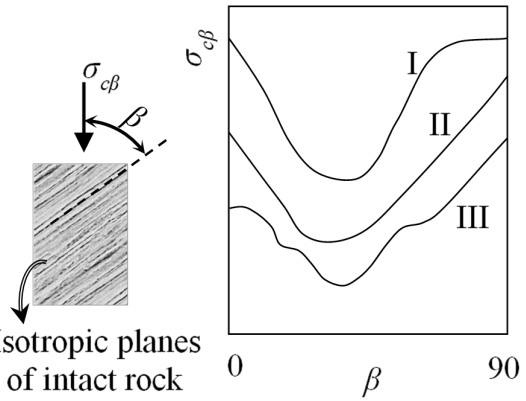

Figure 2. Types of inherent anisotropy of rocks based on the curve of $\sigma_{c\beta}$ versus β: Curve 'I'- Shoulder type, Curve 'II'- U-shaped, Curve 'III'- Wavy [After 15].

2.2. Degree of anisotropy

The degree of anisotropy has been introduced as an indicator to describe the rocks' anisotropy, quantitatively. Several methods are available to determine the degree of anisotropy. Ramamurthy [22] has defined an index, represented by $I\sigma_c$, as the ratio of the maximum uniaxial compressive strength to the minimum uniaxial compressive strength of the intact rocks. Based on this index, he has divided the rocks into five classes ranging from isotropic to very highly anisotropic. Franklin [24] has defined another strength anisotropy index, $I_{a(50)}$, based on the ratio of point load strength index in parallel with, $I_{a(50)h}$, and perpendicular to the bedding planes, $I_{a(50v)}$. Also, the velocity anisotropy index, *VA*, has been proposed by Tsidzi [25] based on the ultrasonic wave velocities in two perpendicular directions. Saroglou *et al*. [26] and Saroglou and Tsiambaos [27] have investigated the inherent anisotropy of metamorphic rocks to determine the degree of anisotropy. They have proposed two classifications for the degree of anisotropy based on the uniaxial compressive strength and the ultrasonic wave velocity. The current anisotropy criteria used in the literature are summarized and presented in Table 2.

Table 2. Current anisotropy criteria of rocks.

Base of classification	UCS	UCS	Point load strength	Ultrasonic wave velocity	Ultrasonic wave velocity
Designated index	$I\sigma_c$	$I\sigma_c^*$	$Ia_{(50)}$	*VA* (%)	I_{vp}
Reference	[22]	[27]	[24]	[25]	[27]
Isotropic	1.0–1.1	1.0–1.1	1.0	< 2.0	-
Fairly anisotropic	1.1–2.0	1.1–2.0	1.0–2.0	2.0–6.0	≤ 1.5
Moderately anisotropic	2.0– 4.0	2.0–3.0		6.0–20.0	1.5–2.0
Highly anisotropic	4.0–6.0	3.0–5.0	2.0–4.0	20.0–40.0	> 2.0
Very highly anisotropic	> 6.0	> 5.0	> 4.0	> 40.0	-

2.3. UCS of transversely-isotropic rocks

For the case of rocks with intrinsic strength anisotropy, it is necessary to determine their strength in an anisotropic manner. Many researchers have proposed equations to describe the dependency of UCS of intact rocks to the angle

of orientation of isotropic planes (Table 3). However, the application of each one of these equations is limited to a particular rock type due to the wide range of geological uncertainties and the limited number of conducted laboratory tests. Hence, it is more convenient to determine the anisotropic rock strength for each individual project. To do so, the uniaxial compressive strength/point load tests must be carried out on the extracted samples in the desired directions. In this case, the UCS of intact rocks can be well-described in the form of the following general equation, which has been initially proposed by Jaeger [28] and later modified by Donath [29]:

$$\sigma_{c\beta} = A - D[\cos 2(\beta_m - \beta)] \quad (1)$$

where β is the angle between the loading direction and the isotropic planes of the intact rock, β_m is the angle at which the uniaxial compressive strength has its minimum value (usually between 30° and 45°), and A and D are constants. The constants A and D can be determined if UCS is known at least at three different loading angles, preferably at β = 0°, 30°, and 90°. In other words, to obtain A and D for any particular case, at least three uniaxial compression tests must be conducted on the rock samples with the aforementioned orientations. The results of the laboratory tests on some anisotropic rock samples and their corresponding fitted strength curves are depicted on Figure 3.

Table 3. Available equations proposed by various researchers to estimate UCS of transversely-isotropic rocks.

Reference	Rock Type		Relation
Jaeger [28] equation modified by Donath [29]	Schistose/foliated/ bedded metamorphic and sedimentary rocks		$\sigma_{c\beta} = A - D[\cos 2(\beta_m - \beta)]$
Ajalloeian and Lashkaripour [21]	Siltshale	$0° \le \beta \le 30°$	$\sigma_{c\beta} = 60.308 - 50.374\ [\cos 2(30 - \beta)]$
		$30° < \beta \le 90°$	$\sigma_{c\beta} = 50.032 - 34.089\ [\cos 2(30 - \beta)]$
	Mudshale	$0° \le \beta \le 30°$	$\sigma_{c\beta} = 79.488 - 60.734\ [\cos 2(30 - \beta)]$
		$30° < \beta \le 90°$	$\sigma_{c\beta} = 43.875 - 25.120\ [\cos 2(30 - \beta)]$
Singh [16]	Schistose rocks		$\sigma_{c\beta} = 473.73 - 0.6\ quartz(\%) + 0.3\ feldspar(\%) - 0.75\ mica(\%) - 0.89\ cholorite(\%) - 0.6\ clay(\%) - 0.08\ grain\ size - 0.09\ area\ weighting - 0.01\ aspect\ ratio - 0.2\ form\ factor + 0.26\ orientation$
Garagon and Can [30]	Laminated sandstones		$\sigma_{c\beta} = -290.73 - 0.46\beta + 0.01\beta^2 - 0.00005\beta^3 + 12.90\gamma$
			$\sigma_{c\beta} = 50.38 - 0.52\beta + 0.01\beta^2 - 0.00006\beta^3 - 6.25n + 0.27n^2$

In these equations: $\sigma_{c\beta}$ is the uniaxial compressive strength (MPa) at angle β relative to the isotropic planes, β_m is the angle at which the uniaxial compressive strength has its minimum value, A and D are constants, γ is the unit weight (kN/m^3), and n is the porosity (%).

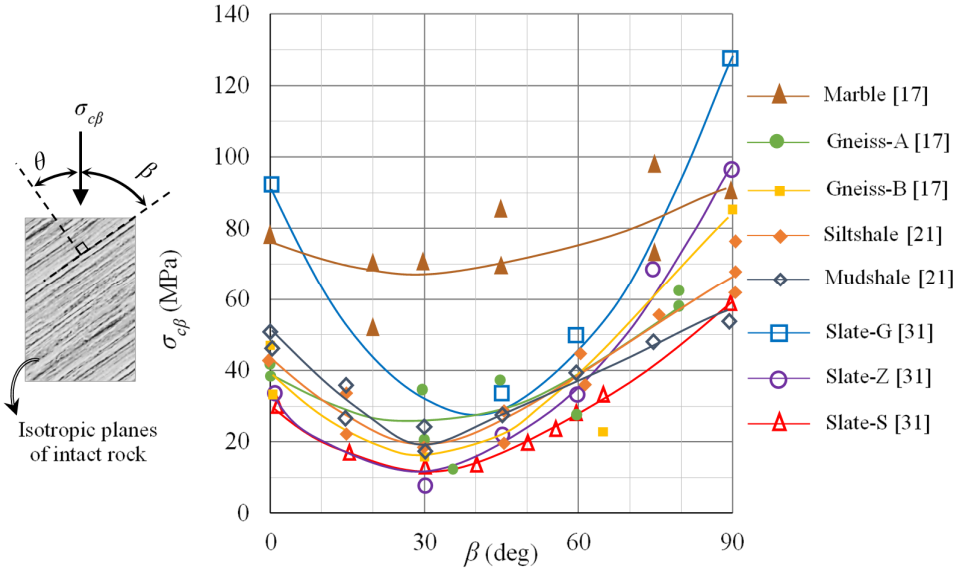

Figure 3. Uniaxial compressive strength of some intact rocks with linear/planar grain structure; the laboratory data and the fitted curves are based on Equation 1 [the data has been extracted from 17, 21, 31].

3. Directional calculation of *UCS*

3.1. *UCS* along arbitrary direction *i*

For site characterization, UCS must be estimated for the desired direction(s). For this purpose, UCS_i is introduced, which represents UCS along with an arbitrary *i*-direction within the 3D space. To calculate UCS_i based on Equation 1, the angle β between the arbitrary *i*-direction and the isotropic planes of the intact rock must be obtained. Instead of β, its complementary angle, θ, can be obtained using the vector analysis. For this purpose, the arbitrary direction can be defined by a unit vector **v**, whose components in the global Cartesian coordinate system, v_X, v_Y, v_Z, are given as follow (Figure 4):

$$v_X = \sin\rho\cos\psi \tag{2}$$

$$v_Y = \cos\rho\cos\psi \tag{3}$$

$$v_Z = \sin\psi \tag{4}$$

where, ρ and ψ are the trend and the plunge of the arbitrary direction, respectively.

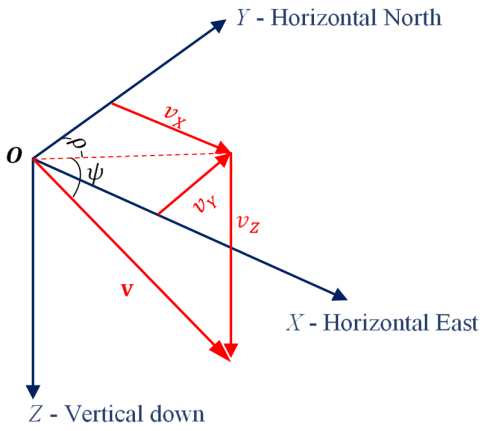

Figure 4. Definition of an arbitrary direction for site characterization as a unit vector and its components in the global Cartesian coordinates.

For the aforementioned case of rocks with linear/planar grain structure, the isotropic plane of intact rock can also be described by its normal vector $\mathbf{u^{ip}}$, whose components in the global Cartesian coordinate system, u_X^{ip}, u_Y^{ip}, u_Z^{ip}, are given as follow:

$$u_X^{ip} = \sin\rho^{ip}\cos\psi^{ip} \tag{5}$$

$$u_Y^{ip} = \cos\rho^{ip}\cos\psi^{ip} \tag{6}$$

$$u_Z^{ip} = \sin\psi^{ip} \tag{7}$$

where, ρ^{ip} and ψ^{ip} are the trend and the plunge of the pole of the isotropic plane, respectively, and are related to the dip direction and the dip of isotropic plane ($DipDir^{ip}$/Dip^{ip}) by the following equations:

$$\rho^{ip} = \begin{cases} DipDir^{ip} + 180° & (for\ DipDir^{ip} < 180°) \\ DipDir^{ip} - 180° & (for\ DipDir^{ip} \geq 180°) \end{cases} \tag{8}$$

$$\psi^{ip} = 90° - Dip^{ip} \tag{9}$$

Substituting Equations. 8 and 9 into Equations. 5-7 yields the following relations for the components of $\mathbf{u^{ip}}$:

$$u_X^{ip} = -\sin(Dip^{ip}).\sin(DipDir^{ip}) \tag{10}$$

$$u_Y^{ip} = -\sin(Dip^{ip}).\cos(DipDir^{ip}) \tag{11}$$

$$u_Z^{ip} = \cos(Dip^{ip}) \tag{12}$$

Then, the angle θ_i^{ip} between the normal to the isotropic plane and the arbitrary *i*-direction can be calculated as follows:

$$\cos\theta_i^{ip} = u_X^{ip}.v_X + u_Y^{ip}.v_Y + u_Z^{ip}.v_Z \tag{13}$$

Thus, by substituting Equations. 2-4 and 10-12 into Equation 13, and considering that θ_i^{ip} is in the range of 0°-90°, the following relation is obtained to calculate θ_i^{ip} for the prescribed *i*-direction:

$$\theta_i^{ip} = \cos^{-1}\left|\cos(Dip^{ip})\sin\psi - \sin(Dip^{ip})\cos\psi\cos(DipDir^{ip} - \rho)\right| \tag{14}$$

Then, bearing in mind that θ_i^{ip} and β are complementary angles, UCS_i can be calculated for the prescribed *i*-direction by substituting $\beta = 90 - \theta_i^{ip}$ into Equation 1, which leads to the following relation:

$$UCS_i = A + D\left[\cos 2\left(\beta_m + \theta_i^{ip}\right)\right] \tag{15}$$

Using this equation, it is possible to calculate UCS of intact rocks along with any desired direction by means of orientation of isotropic planes that are recorded during geological mapping. It is worth noting that in the case of transversely-isotropic rocks, the directions located at a particular angle of β exhibit the same *UCS*. In a 3D space, these directions lay on a cone around the normal to the isotropic planes (see Figure 5 for the case of β = 60°). This causes a symmetry on the values of UCS_i around the normal vector to the isotropic planes.

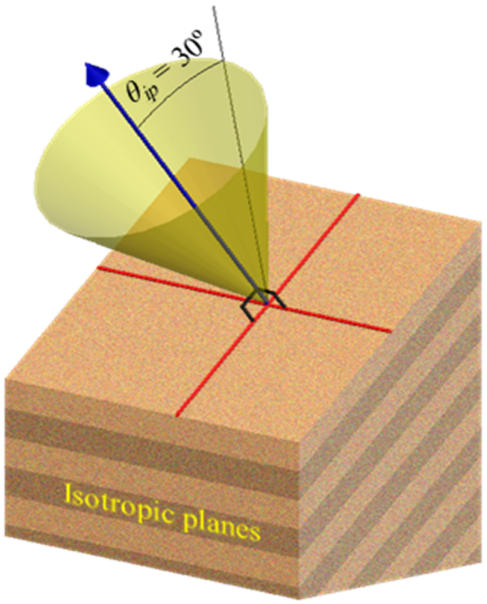

Figure 5. Cone of directions with an angle of θ_{ip} = 30° with the normal to isotropic planes (β = 90°-θ_{ip} = 60°).

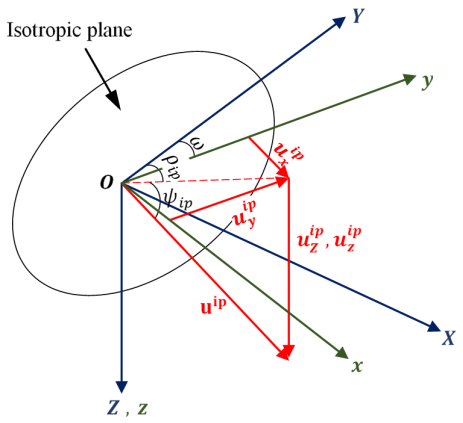

Figure 6. Normal vector of isotropic plane, $\mathbf{u^{ip}}$, and its components in local coordinates (rotation of horizontal *x* and *y* axes around Z-axis).

3.2. *UCS* along global Cartesian coordinate system

In some cases, the desired directions may coincide with the global Cartesian coordinate system. In this case, by recalling Equation 14, after substitution for **v** components and simplification, results the following:

$$\theta_X^{ip} = \cos^{-1}\left|\sin(Dip^{ip})\sin(DipDir^{ip})\right| \quad (16)$$

$$\theta_Y^{ip} = \cos^{-1}\left|\sin(Dip^{ip})\cos(DipDir^{ip})\right| \quad (17)$$

$$\theta_Z^{ip} = \cos^{-1}\left|\cos(Dip^{ip})\right| \quad (18)$$

By substituting the resulting Equations. 16-18 into Equation 15 for θ_i^{ip}, the uniaxial compressive strength, UCS_i, along the global axes can be determined.

3.3. *UCS* along a local Cartesian system rotated around Z-axis

In most cases, the desired directions are not consistent with the global Cartesian coordinate system. Therefore, a local coordinate system must be introduced. In this case, a horizontal plane with *x* and *y* axes is presumed rotating around the *Z*-axis at ω degree (Figure 6). In this system, the components of normal vector of isotropic planes of intact rock, $\mathbf{u^{ip}}$, will be as follow:

$$u_x^{ip} = \sin(\rho_{ip} - \omega)\cos\psi_{ip} \quad (19)$$

$$u_y^{ip} = \cos(\rho_{ip} - \omega)\cos\psi_{ip} \quad (20)$$

$$u_z^{ip} = u_Z^{ip} = \sin\psi_{ip} \quad (21)$$

Therefore, in this case, Equations. 16-18 are modified as follow:

$$\theta_x^{ip} = \cos^{-1}\left|\sin(Dip^{ip})\sin(DipDir^{ip} - \omega)\right| \quad (22)$$

$$\theta_y^{ip} = \cos^{-1}\left|\sin(Dip^{ip})\cos(DipDir^{ip} - \omega)\right| \quad (23)$$

$$\theta_z^{ip} = \cos^{-1}\left|\cos(Dip^{ip})\right| \quad (24)$$

One can substitute the results of Equations. 22-24 into Equation 15 for θ_i^{ip} to determine the directional uniaxial compressive strength, UCS_i, along the local axes.

3.4. All-round calculations and illustration of UCS_i

By implementing the aforementioned mathematical formulation, the UCS_i value(s) can be calculated at any arbitrary direction(s). However, the method is capable of providing a continuous all-round distribution of UCS_i as well.

For this purpose, a proper net of Trend-Plunge values is required to cover all the probable spatial directions. An interval of 5 to 10 degrees of Trend-Plunge values can provide the necessary network. Then, by calculating UCS_i for the nodes of this network, its spatial distribution will be obtained. For this purpose, calculations can be carried out simply by using a spreadsheet. In order to achieve the most desired representative distribution, it is suitable to use the lower hemisphere Stereonet. Therefore, UCS_i can be presented in the form of its contour-plot on a Stereonet. This type of presentation provides a quantitative all-round visualization of UCS of intact rocks. Hence, the rock's strength anisotropy and the directions of the highest and the lowest compressive strength can be well-characterized. The procedure for all-round calculations and representation of UCS_i will be discussed by a case study in Section 4.

4. A practical case study

To illustrate the application of the proposed formulation in describing the strength of transversely-isotropic rocks, a practical example is given in this section. The field data is taken from the Kanigoizhan dam site, located 22.5km southwest of Baneh, Kurdistan Province, Iran. The dam and its water transmission system are under study to transfer water from the Chouman and Bashavan rivers to the towns of Baneh and Saqqez. The Kanigoizhan dam, with a height of 122m from the foundation level, will have a reservoir capacity of 133 million cubic meters.

A wide area of the dam site is composed of Cretaceous metamorphic phyllites, which is the oldest rock unit in the studied area. The dam body and the corresponding reservoir are located on this rock unit. The metamorphosis processes on these phyllites resulted in the formation of foliations. The orientation of these foliations is variable due to tectonic activities. However, in general, their dip direction is N039E and their dip is about 37 degrees (Figure 7).

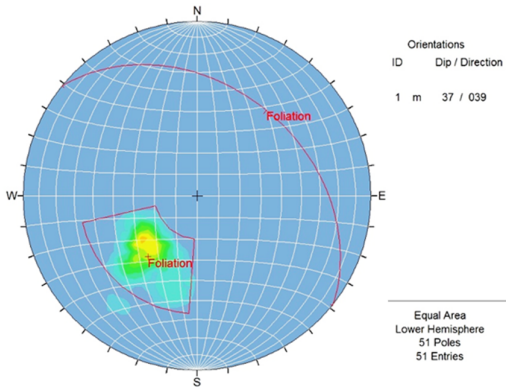

Figure 7. Stereonet representation of the mapped foliations at the Kanigoizhan dam site, Kurdistan, Iran.

At the dam site, the river flows in a direction with azimuth of 230 degrees. The general layout of the dam components is represented in Figure 8. As it can be seen in this figure, different structures of the dam have different orientations regarding the general direction of the foliation planes. Therefore, the rock anisotropy can have significant effects on the behavior of each one of these structures, and must be carefully considered during the design process.

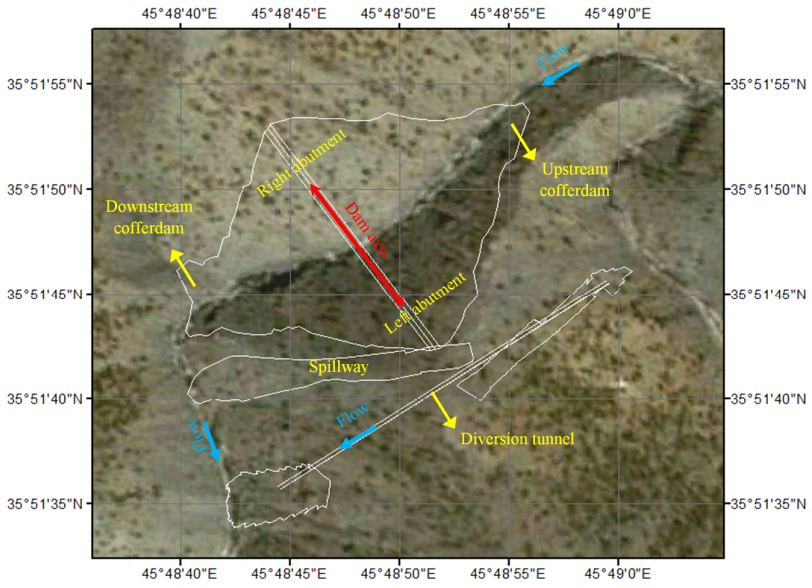

Figure 8. General layout of the Kanigoizhan dam structures, Kurdistan, Iran.

In the second phase studies, a special attention was paid to the characterization of rock anisotropy during the rock mechanical tests. For this purpose, several boreholes at different angles to the foliation planes were drilled within an exploration gallery. To determine UCS of the phyllite rock, 37 oriented specimens have been tested. The pre-test and post-test pictures of one of the specimens, in which angle β between the foliation planes and the loading direction is 65°, are shown in Figure 9.

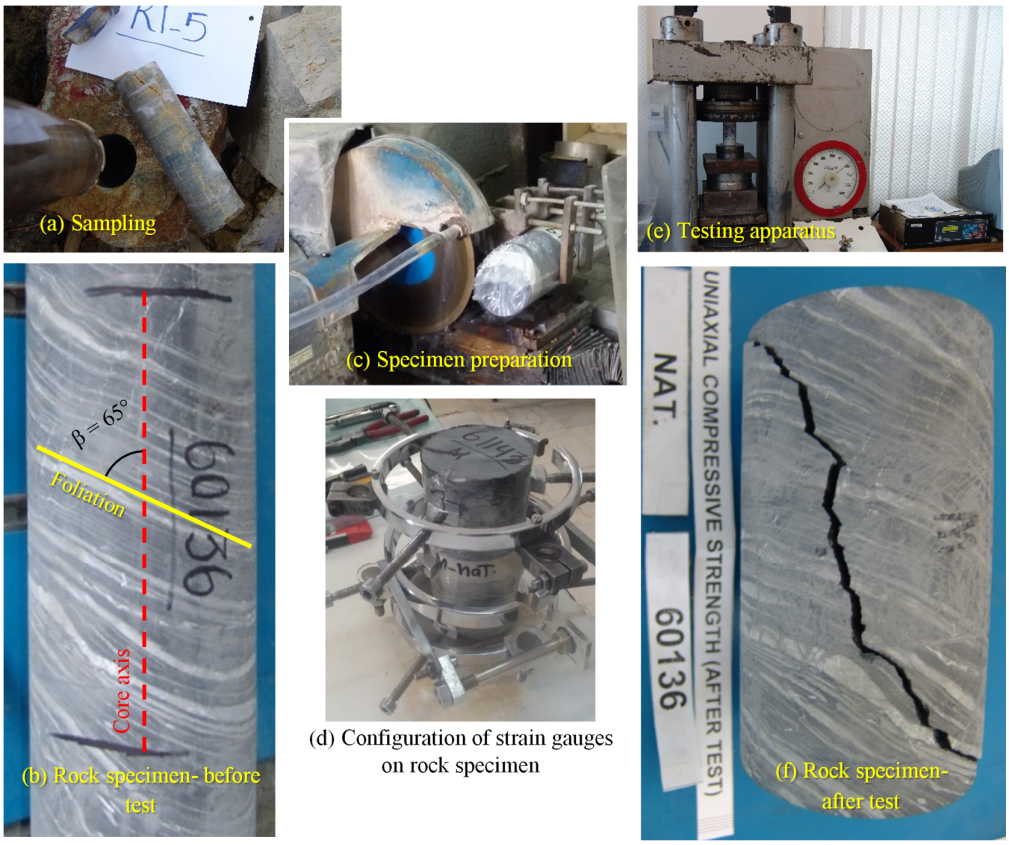

Figure 9. Uniaxial compression test on a phyllite core specimen taken from the Kanigoizhan dam site, Kurdistan, Iran.

The results of the laboratory uniaxial compression tests are depicted in Figure 10 in the form of $\sigma_{c\beta}$ versus β. To characterize the anisotropic UCS of intact rocks, three different equations have been fitted to the laboratory data based on the general relationship proposed by Donath [29]. These equations for the maximum, average, and minimum values of $\sigma_{c\beta}$ are given bellow:

$$\sigma_{c\beta}^{Max} = 57 - 21.6[\cos 2(25 - \beta)] \quad (25)$$

$$\sigma_{c\beta}^{Ave} = 38.6 - 13.3[\cos 2(35 - \beta)] \quad (26)$$

$$\sigma_{c\beta}^{Min} = 26.7 - 11[\cos 2(44 - \beta)] \quad (27)$$

As it can be seen in Figure 10, the laboratory data is scattered, which could be due to the lithological variations. With regard to the actual range of variation of laboratory data, estimation of the average values of $\sigma_{c\beta}$ by Equation 26 is accompanied with an error of 1~19 MPa. Hence, it is more proper to take the statistical distribution of $\sigma_{c\beta}$ into account by the set of equations 25-27.

According to Equation 15, adjustment of Equations. 25-27 for a 3D space will be as follows:

$$UCS_i^{Max} = 57 + 21.6[\cos 2(25 + \theta_i^{ip})] \quad (28)$$

$$UCS_i^{Ave} = 38.6 + 13.3[\cos 2(35 + \theta_i^{ip})] \quad (29)$$

$$UCS_i^{Min} = 26.7 + 11[\cos 2(44 + \theta_i^{ip})] \quad (30)$$

Comparison of the curves in Figure 10 with the criteria presented in Table 1 and also with the curves in Figure 2 demonstrates that the strength anisotropy of the understudied phyllite rock is U-shaped. As mentioned earlier, this is the characteristic of metamorphic rocks that contain one set of cleavage. Also, according to Table 2, this rock is to be classified as a moderately anisotropic rock.

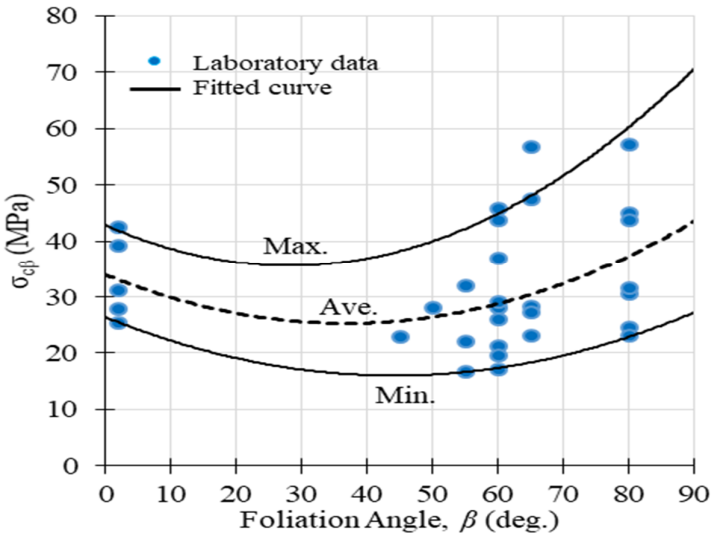

Figure 10. Data of laboratory uniaxial compression tests on oriented rock samples and the fitted $\sigma_{c\beta} - \beta$ curves for a transversely-isotropic phyllite, obtained from the Kanigoizhan dam site, Kurdistan, Iran.

One of the key aspects of the design analysis could be the bearing capacity of the dam's foundation and stability analysis of the corresponding abutments. Hence, it would be desirable to calculate UCS_i for the directions parallel with and perpendicular to the dam's abutments. The azimuth of Kanigoizhan dam's abutments is 231°. Upon this, a local Cartesian coordinate system has been defined, as described in Section 3-3, by an angle of rotation of ω = 231°. In this coordinate system, the *x*-axis and *y*-axis are parallel with and perpendicular to the dam's abutments, respectively, while the *z*-axis denotes vertical-down. By means of Eqns. 22-24, the angles θ_x^{ip}, θ_y^{ip}, and θ_z^{ip} could be obtained for the prescribed directions. Then, substituting these values into Equations. 28-30 yields the corresponding values of UCS_i. The results obtained are summarized in Table 4.

Table 4. Determination of UCS_i for a transversally-isotropic phyllite obtained from the Kanigoizhan dam site, Kurdistan, Iran.

Direction (*i*)		θ_i^{ip} (deg)	β (deg)	UCS_i (MPa)		
				Max.	Ave.	Min.
x	(Perpendicular to dam's abutments)	83	7	39	31	24
y	(Parallel with dam's abutments)	54	36	37	25	16
z	(Vertical-down)	37	53	45	28	16

On the other hand, one of the key features of the proposed method is to demonstrate the all-round spatial distribution of UCS_i on a Stereonet. The procedure is as discussed in Section 3.4. To calculate the all-round values of UCS_i, a spreadsheet has been used. The network selected to cover all possible directions consists of trend values from 0° to 360° and plunge values from 0° to 90°, each of them with an interval of 5 degrees. For each node of the network, which actually represents an arbitrary spatial direction, θ_i^{ip} has been calculated using Equation 14. Then, the values of the maximum, average, and minimum UCS_i have been calculated for each node of the network by means of Equations. 28-30. Accordingly, the contour-plots of the maximum, average, and minimum UCS_i have been obtained and depicted in Figure 11. This figure shows that the highest values of UCS_i are placed on the direction of 219°/53° (trend/plunge), which is perpendicular to the isotropic planes of intact rock. Furthermore, at each plot, the lowest value of UCS_i forms two bands around the great circle of isotropic planes. The angle between these bands and the great circle of isotropic planes are 44°, 35°, and 25° for the contour-plots of the minimum, the average, and the maximum UCS_i, respectively. Actually, these angles are the same as the values of β_m that have been determined through the process of curve fitting to obtain Equations. 25-27.

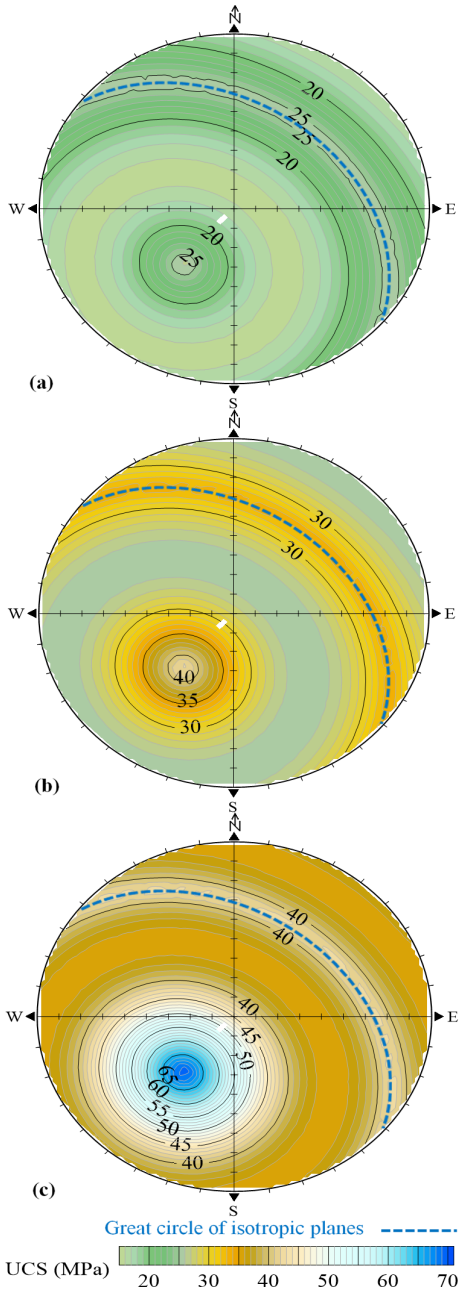

Figure 11. Contour-plots of a) minimum, b) average, and c) maximum UCS_i for the phyllite rock of the Kanigoizhan dam site, Kurdistan, Iran.

More detailed investigations on the variations of UCS_i can be carried out by 2D graphs. For this purpose, this type of graph can be provided along the critical and or the desired directions. For example, variations of UCS_i in a cross-section perpendicular to the dam axis is substantial for analysis of the bearing capacity of dam foundation. For the current case study, graphs of variations of UCS_i along the N39E-S39W, N-S, and S51E-N51W directions have been provided and depicted in Figure 12. On each graph of this figure, the diagrams of the minimum, average, and maximum UCS_i are shown. These diagrams are consistent with the contour-plots of Figure 11.

Figure 12b illustrates the variations of UCS_i in a cross-section perpendicular to the dam axis (parallel with the dam abutments). This graph can be used in the analysis of the bearing capacity of the dam's foundation and stability of the portals of diversion tunnel as well. As it can be seen, this graph exhibits the highest strength variations. This indicates the importance of taking the strength anisotropy into account during the aforesaid analysis.

Figure 12c illustrates the variations of UCS_i in the N-S cross-section as an arbitrary direction. This direction has an angle of 51° relative to the dam axis. The variations of UCS_i along this direction is less than those in Figure 12b. Furthermore, the variations of UCS_i in a cross-section parallel with the dam axis (perpendicular to the dam abutments) are shown on Figure 12d. This graph is helpful to be used for analysis of stability of the dam abutments and the diversion tunnel. The smoother shape of this graph indicates the lower strength anisotropy along this direction.

As mentioned earlier, in all graphs of Figure 12, the statistical distribution of UCS_i is shown by the diagrams of its maximum, average, and minimum values. Accordingly, depending on the aim of analysis, the proper values of UCS_i can be selected by the designer.

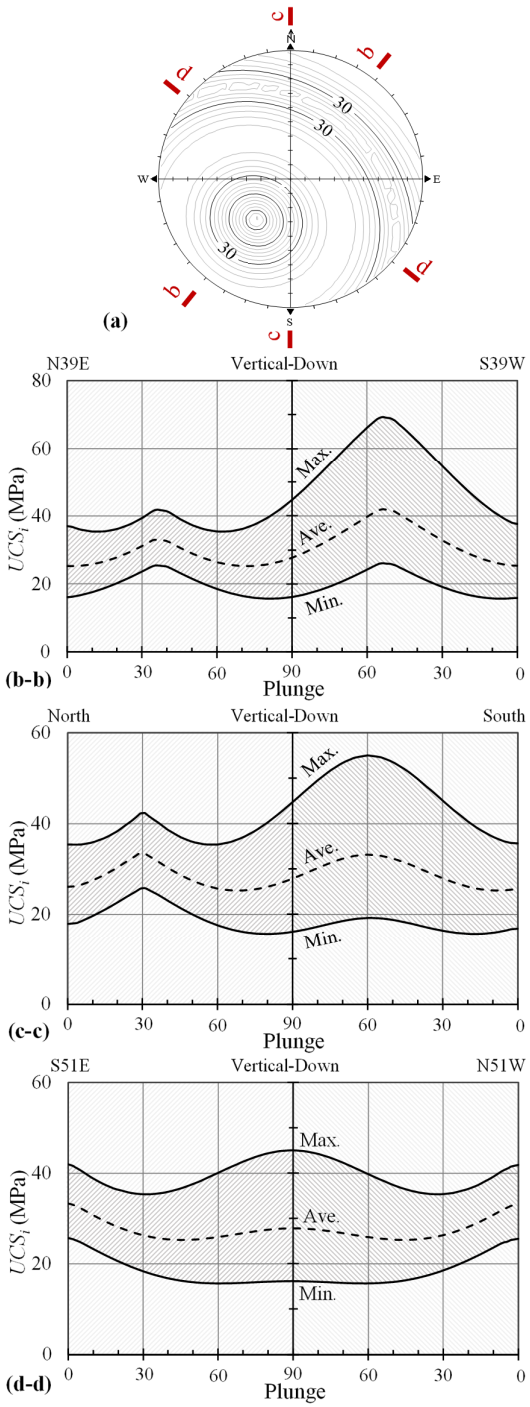

Figure 12. Detailed analysis of UCS of transversely-isotropic phyllite rock of the Kanigoizhan dam site, Kurdistan, Iran; a) Alignments of 2D sections on the contour-plots of average UCS_i. b-b, c-c, and d-d) Graphs of UCS_i variations along with sections; N39E-S39W, N-S, and S51E-N51W directions, respectively.

5. Conclusions

In this paper, a semi-empirical method has been proposed for a 3D characterization of the uniaxial compressive strength (UCS) of transversely-isotropic intact rocks. For this purpose, UCS_i was defined as the UCS along an arbitrary direction '*i*'. Based on the proposed formulation, one can obtain the all-round distribution of UCS_i as well as its particular values along any arbitrary direction. For a proper evaluation of UCS_i, an all-round representation has been proposed in the form of its contour-plot on a lower hemisphere Stereonet. This representation provides a good perception into the spatial distribution of UCS of intact rocks. The results of the all-round calculations can also be used for a detailed analysis of UCS_i in the form of 2D graphs along any desired alignment.

Application of the proposed method was illustrated by an actual case study from the Kanigoizhan dam site, located in the Kurdistan Province (Iran). The results of the laboratory analysis showed that the phyllite rock type of this site had a U-shaped type anisotropy. Implementation of the proposed method for this site revealed that a longitudinal section perpendicular to the dam axis exhibits the most critical anisotropic behavior. This indicates the importance of taking the rock's anisotropy into account when analyzing the bearing capacity of the dam' foundation and the stability of the portals of diversion tunnel. Finally, the results of the given case study illustrated the applicability of the method as a practical tool for an in-situ rock characterization.

Acknowledgment

The authors wish to express their gratitude to 'Sadd Tunnel Pars' Consulting Engineers Co. for kind cooperation in providing the field data.

References

[1]. Al-Karni, A.A. and Al-Shamrani, M.A. (2000). Study of the effect of soil anisotropy on slope stability using method of slices. Comput. Geotech. 26: 83–103.

[2]. Majdi, A. and Amini, M. (2008). Effects of geostructural weaknesses on flexural toppling, Proc, Fifth Asian Rock Mechanics Symposium (ARMS5), Tehran, 24-26 November, 611–618.

[3]. Majdi, A. and Amini, M. (2011). Analysis of geo-structural defects in flexural toppling failure. Int. J. Rock Mech. Min. Sci. 48: 175–186.

[4]. Majdi, A. and Hassani, F. (1989). Access tunnel convergence prediction in longwall coal mining. Int. J. Min. Geol. Eng. 7: 283–300.

[5]. Satici, O. and Ünver, B. (2015). Assessment of tunnel portal stability at jointed rock mass: A comparative case study. Comput. Geotech. 64: 72–82.

[6]. Barton, N. and Quadros, E. (2014). Most rock masses are likely to be anisotropic. Proc, Rock

Mechanics for Natural Resources and Infrastructure-ISRM Specialized Conference. CBMR/ABMS and ISRM, Goiania, 9-13 September.

[7]. Wittke, W. (2014). Rock mechanics based on an anisotropic jointed rock model (AJRM), Wiley Blackwell, Berlin, 875 P.

[8]. Donath, F.A. (1964). Strength variation and deformational behavior in anisotropic rock. In: Judd, W. (Ed.) State of Stress in the Earth's Crust, New York, pp. 281–298.

[9]. Hoek, E. (1964). Fracture of anisotropic rock. J. South African Inst. Min. Metall. 64: 501–518.

[10]. McLamore, R. and Gray, K.E. (1967). The mechanical behavior of anisotropic sedimentary roks. J. Eng. Ind. 89: 62–76.

[11]. Attewell, P.B. and Sandford, M.R. (1974). Intrinsic shear strength of a brittle, anisotropic rock- I: Experimental and mechanical interpretation. Int. J. Rock Mech. Min. Sci. Geomech. Abstr. 11: 423–430.

[12]. Brown, E.T., Richards, L. and Barr, M. (1977). Shear strength characteristics of Delabole slates. Proc, Conference on Rock Engineering, New Castle Upon Tyne, 33–55.

[13]. McCabe, M.W. and Koerner, R.M. (1975). High pressure shear strength investigation of an anisotropic mica schist rock. Int. J. Rock Mech. Min. Sci. Geomech. Abstr. 12: 218–228.

[14]. Nasseri, M.H., Rao, K.S. and Ramamurthy, T. (1997). Failure mechanism in schistose rocks. Int. J. rock Mech. Min. Sci. Geomech. Abstr. 34: 460.

[15]. Nasseri, M.H.B., Rao, K.S. and Ramamurthy, T. (2003). Anisotropic strength and deformation behavior of Himalayan schists. Int. J. Rock Mech. Min. Sci. 40: 3–23.

[16]. Singh, V.K., Singh, D. and Singh, T.N. (2001). Prediction of strength properties of some schistose rocks from petrographic properties using artificial neural networks. Int. J. Rock Mech. Min. Sci. 38: 269–284.

[17]. Saroglou, H. and Tsiambaos, G. (2008). A modified Hoek- Brown failure criterion for anisotropic intact rock. Int. J. Rock Mech. Min. Sci. 45: 223–234.

[18]. Ramamurthy, T., Rao, G. and Singh, J. (1988). A strength criterion for anisotropic rocks, Proc, Fifth Australia-New Zealand Conference on Geomechanics, Sydney, 22-26 August, 253–257.

[19]. Al-Harthi, A.A. (1998). Effect of planar structures on the anisotropy of Ranyah sandstone, Saudi Arabia. Eng. Geol. 50: 49–57.

[20]. Colak, K. and Unlu, T. (2004). Effect of transverse anisotropy on the Hoek-Brown strength parameter "mi" for intact rocks. Int. J. Rock Mech. Min. Sci. 41: 1045–1052.

[21]. Ajalloeian, R. and Lashkaripour, G.R. (2000). Strength anisotropies in mudrocks. Bull. Eng. Geol. Environ. 59: 195–199.

[22]. Ramamurthy, T. (1993). Strength and modulus responses of anisotropic rocks. In: Brown, E.T. (Ed.), Comprehensive rock engineering. Pergamon press, pp. 313–329.

[23]. Singh, K.B. and Singh, T.N. (1998). Ground movements over longwall workings in the Kamptee coalfield, India. Eng. Geol. 50: 125–139.

[24]. Franklin, J.A. (1985). Suggested method for determining point load strength. Int. J. Rock Mech. Min. Sci. Geomech. Abstr. 22: 51–60.

[25]. Tsidzi, K.E.N. (1997). Propagation characteristics of ultrasonic waves in foliated rocks. Bull. Int. Assoc. Eng. Geol. 56: 103–114.

[26]. Saroglou, H., Marinos, P. and Tsiambaos, G. (2003). The anisotropic nature of selected metamorphic rocks from Greece. Proc, ISRM 2003-Technology roadmap for rock mechanics. South African Institute of Mining and Metallurgy, 8-12 September, 1019–1024.

[27]. Saroglou, H. and Tsiambaos, G. (2007). Classification of anisotropic rocks. Proc, 11th Congress of the International Society for Rock Mechanics, Lisbon, 09-13 July, 191–196.

[28]. Jaeger, J.C. (1960). Shear failure of anisotropic rocks. Geol. Mag. 97: 65–72.

[29]. Donath, F.A. (1961). Experimental study of shear failure in anisotropic rocks. Geol. Soc. Am. Bull. 72: 985–990.

[30]. Garagon, M. and Can, T. (2010). Predicting the strength anisotropy in uniaxial compression of some laminated sandstones using multivariate regression analysis. Mater. Struct. 43: 509–517.

[31]. Saeidi, O., Rasouli, V., Geranmayeh Vaneghi, R. and Gholami, R. (2014). A modified failure criterion for transversely isotropic rocks. Geosci. Front. 5: 215–225.

مشخصه‌سازی سه بعدی مقاومت فشاری تک محوره سنگ‌های بکر شبه‌همسانگرد

وحید معاذاللهی و عباس مجدی*

1- دانشکده مهندسی معدن، پردیس دانشکده‌های فنی، دانشگاه تهران، تهران، ایران

ارسال 2019/10/19، پذیرش 2020/04/02

* نویسنده مسئول مکاتبات: amajdi@ut.ac.ir

چکیده:

مقاومت فشاری تک محوره (UCS) سنگ‌های بکر یکی از پارامترهای کلیدی در مشخصه‌سازی هر ساختگاه سنگی است. وضعیت همسانگردی/ناهمسانگردی UCS سنگ‌های بکر به ساختار داخلی آنها وابسته است. سنگ‌های با ساختار دانه‌ای تصادفی، رفتار همسانگرد نشان می‌دهند. در حالیکه، رفتار سنگ‌های با ساختار دانه‌ای خطی/ صفحه‌ای عموماً شبه‌همسانگرد است. در حالت اخیر، UCS سنگ بکر با یک سری آزمایش‌های آزمایشگاهی بر روی نمونه‌های سنگی جهت‌یافته تعیین می‌شود. روابط تجربی متعددی برای توصیف مقاومت این گونه سنگ‌ها وجود دارد. علیرغم اینکه مشخصه‌سازی سنگ‌های شبه‌همسانگرد عملاً یک مسأله سه بعدی است، اما این روابط تنها یک توصیف دو بعدی از UCS این سنگ‌ها فراهم می‌کنند. بنابراین، در این مقاله روشی برای توصیف کمی سه بعدی UCS سنگ‌های بکر شبه‌همسانگرد ارائه شده است. با استفاده از این روش، UCS را می‌توان در هر راستای فضایی دلخواه تعیین کرد. همچنین، برای نمایش توزیع فضایی UCS، روشی مبتنی بر ترسیم کنتورپلات مقادیر آن بر روی استرونت نیمکره پایین ارائه شده است. روش پیشنهادی بر روی یک مطالعه موردی واقعی برگرفته از ساختگاه سد کانی‌گویژان در استان کردستان (ایران) بکار گرفته شده است. نتایج حاصل از کاربرد این روش بر روی سنگ فیلیت ساختگاه مذکور حاکی از آن است که راستای عمود بر محور سد بیشترین رفتار ناهمسانگرد را نشان می‌دهد. بنابراین، در نظر گرفتن ویژگی ناهمسانگردی سنگ در تحلیل‌های مرتبط با این راستا اهمیت فراوانی دارد. نتایج بدست آمده، همراه با توزیع آماری UCS، رویکردی عملی برای انتخاب مقادیر مناسب UCS براساس هدف تحلیل‌های مد نظر فراهم می‌سازد.

کلمات کلیدی: سنگ بکر، مقاومت فشاری تک محوره، شبه‌همسانگرد، مشخصه‌سازی سه بعدی، استرونت.